Biophysical Chemistry 148 (2010) 138–143

Contents lists available at ScienceDirect

Biophysical Chemistry

journal homepage: http://www.elsevier.com/locate/biophyschem

Real-time detection of DNA cleavage induced by $[M(2,2'\text{-dipyridylamine})_2(NO_3)_n]^{x+}$ ($M = Cd, Cu, Ni, Zn$, $n = 1,2$, $x = 0,1$): Effect of central metal ions

Kyeung Joo Jang [a], Ga-Young Yeo [a], Tae Sub Cho [a], Geun Hee Eom [b], Cheal Kim [b,*], Seog K. Kim [a,*]

[a] Department of Chemistry, Yeungnam University, Gyeongsan City, Gyeong-buk 712-749, Republic of Korea
[b] Department of Fine Chemistry, Seoul National University of Technology, Seoul 139-743, Republic of Korea

ARTICLE INFO

Article history:
Received 1 February 2010
Received in revised form 10 March 2010
Accepted 11 March 2010
Available online 16 March 2010

Keywords:
DNA cleavage
Linear dichroism
Metal complexes
$[M(Hdpa)(NO_3)_n]^{x+}$
Real-time detection

ABSTRACT

$[M(Hdpa)_2(NO_3)_n]^{x+}$ ($M = Zn^{II}$, Cd^{II}, Cu^{II} and Ni^{II}, $n = 1,2$, and $x = 0, 1$) complexes were synthesized, and their activity as catalysts for DNA cleavage reactions were investigated using electrophoresis and linear dichroism technique (LD). All four metal complexes effectively cleaved pBR322 super-coiled DNA. The electrophoresis analysis showed that the $[Zn(Hdpa)_2(NO_3)]^+$ and $[Cd(Hdpa)_2(NO_3)_2]$ complexes most effectively cleaved the super-coiled DNA, whereas the $[Ni(Hdpa)_2(NO_3)]^+$ complex was least effective. The magnitude of LD in the DNA absorption region reflects the flexibility and length of DNA when the conditions for measurement are properly adjusted. The double stranded DNA cleavage increases the flexibility of DNA and reduces the length, reducing the magnitude of LD in DNA absorption region. Utilizing this LD property, the cleavage was detected in real-time by measuring the LD magnitude with respect to time. The decrease in the LD magnitude was described as the sum of two exponentials. The fast component was tentatively assigned to the cleavage of the single strand, reflecting the increase in the flexibility of DNA, and the slow component was assigned to the cut of the double strand which reduced the length of DNA. The average reaction time was the fastest for the Zn^{II} complex and the slowest for the Ni^{II} complex. The reaction time of the Cd^{II} complex was as fast as that of the Zn^{II} complex. Both the Zn^{II} and Cd^{II} belong to group 12, suggesting that $[M(Hdpa)_2(NO_3)_n]^{x+}$ with central metal ions from group 12 most efficiently cleaved double stranded DNA.

1. Introduction

Metal ions and complexes have large potential in biological applications because of their cationic character, modularity, reactivity, redox chemistry, photoreactions, and precisely defined three dimensional structures. They have been investigated and used as anticancer reagents [1], artificial nuclease [2–4], acceptors or donors in the DNA mediated electron/hole/energy transfer [5–9], and probes for nucleic acids structures [10–13]. The catalytic effects of the various metal complexes on DNA strand breakage through a hydrolytic or oxidative mechanism are well known. Recently, a report showed that the [Cu(*N*-9*H*-purine-6-yl)benzenesulfonamide (phenanthroline)$_2$]·3H$_2$O complex exhibited cleavage activity to plasmid DNA [14] and a different report further studied this behavior [15]. (*N*,*N*′-ethylenediaminediacetato)metal(II) complexes, with metals such as Cu, Co, Ni and Zn, cleaved plasmid DNA in the presence of hydrogen peroxide. Cu was more efficiently cleaved DNA than Zn and Ni. The amount of OH radicals was responsible for different efficiencies.

Typically, the detection method for DNA cleavage is agarose gel electrophoresis. However, this method is not ideal for time-based measurements. Various fluorescence techniques, including fluorescence resonance energy transfer, have been utilized to detect DNA cleavage in real-time [16–19]. The fluorescence techniques also have limitations, including the need to modify DNA with the fluorescent probes in order for the fluorescence techniques to be applicable. Recently, linear dichroism (LD) has been shown to be a powerful alternative technique for the real time detection of both super-coiled and double stranded DNA cleavage [20–22]. LD is the difference in the absorbance of light polarized in directions parallel and perpendicular to the sample orientation axis, and its magnitude in the DNA absorption region depends solely on the length and flexibility of DNA when the other experimental conditions are constant [23–26]. In double stranded DNA, cleavage of one of the strands increases the flexibility of DNA whereas cleavage of both strands result in shortened DNA. Both decrease the LD magnitude in the DNA absorption region. In this study, the LD technique was used for the real-time detection of DNA cleavage induced by newly synthesized $[M(2,2'\text{-dipyridylamine})_2(NO_3)_n]^{x+}$ ($M = Cd, Cu, Ni$ and Zn, $n = 1,2$, $x = 0,1$) metal complexes, and the results were compared to the conventional electrophoresis technique. As an artificial chemical nuclease, new simple series of metal complexes possessing two identical ligands,

* Corresponding authors. Seog K. Kim is to be contacted at Tel.: +82 53 810 2362. Cheal Kim, Tel.: +82 2 970 6693.
E-mail addresses: chealkim@snut.ac.kr (C. Kim), seogkim@yu.ac.kr (S.K. Kim).

0301-4622/$ – see front matter © 2010 Elsevier B.V. All rights reserved.
doi:10.1016/j.bpc.2010.03.009

namely 2,2′-dipyridylamine (referred to as Hdpa) (Fig. 1), were synthesized. The combination of the identical ligands and the real-time LD detection technique were used to compare the effects of the central metal on the reaction time and efficiency of the DNA cleavage reaction.

2. Materials and methods

2.1. Materials

Calf thymus DNA (referred to as DNA) was purchased from Worthington Biochemical Co. (Lakewood, NJ) and was dissolved through gentle shaking in a 5 mM cacodylate buffer, pH 7.0, containing 100 mM NaCl and 1 mM EDTA at 4 °C. The DNA solution was dialyzed several times against pH 7.0 5 mM cacodylate buffer at 4 °C. The latter cacodylate buffer was used throughout this work except for during the electrophoresis work. Super-coiled pBR322 DNA was purchased from Fermentas (Hanover, MD). 2,2′-Dipyridylamine, methanol, acetone, and metal nitrates (metal = Ni, Cu, Zn and Cd) were purchased from Aldrich and used as received in the synthesis of the metal complexes. The concentrations of the DNA was determined using an extinction coefficient of $\varepsilon_{260\ nm} = 6700\ M^{-1}\ cm^{-1}$. The molar extinction coefficients of the synthesized $[M(Hdpa)_2(NO_3)_n]^{x+}$ metal complexes were determined from the absorbance at their maximum of aqueous solution with known concentrations: $\varepsilon_{315\ nm} = 26{,}295\ M^{-1}\ cm^{-1}$, $\varepsilon_{315\ nm} = 26{,}930\ M^{-1}\ cm^{-1}$, $\varepsilon_{315\ nm} = 23{,}855\ M^{-1}\ cm^{-1}$, $\varepsilon_{314\ nm} = 31{,}290\ M^{-1}\ cm^{-1}$ for M = Cd, Cu, Ni and Zn, respectively.

2.2. Synthesis of the metal complexes

The Cd^{II} and Zn^{II} complexes (Fig. 1) were synthesized according to a previously reported method [27,28].

Preparation of the Ni^{II} complex: 74.2 mg (0.25 mmol) of $Ni(NO_3)_2 \cdot 6H_2O$ were dissolved in 4 mL methanol and carefully layered with an acetone solution of 2,2′-dipyridylamine ligand (86.5 mg, 0.5 mmol). A 62.4% yield (81.9 mg) of the Ni^{II} complex was obtained after three days. ^1H NMR (DMSO, 300 MHz): δ 9.64 (s, 1H, N–H) and δ 8.20, 7.70, 7.64 and 6.85 (m, 8H, pyridyl-H). IR (KBr): $\nu(cm^{-1}) = 3301$(m), 3197(m), 1649(s), 1590(s), 1534(s), 1479(s), 1328(brs), 1270(s), 1237(brs), 1161(s), 1055(m), 1016(s), 907(m), 869(m), 770(brs), 673(w), 646(m), 606(w), 533(s), 430(s). Anal. Calcd. for $C_{20}H_{18}NiN_8O_6$ (525.10), 1: C, 45.75; H, 3.46; N, 21.34. Found: C, 45.97; H, 3.77; N, 20.01%.

Preparation of the Cu^{II} complex: 23.9 mg (0.125 mmol) of $Cu(NO_3)_2 \cdot 5/2H_2O$ were dissolved in 4 mL methanol and carefully layered with an acetone solution of 2,2′-dipyridylamine ligand (46.5 mg, 0.25 mmol). A yield of 51.7 % (34.2 mg) of the Cu^{II} complex was obtained after one week. IR (KBr): $\nu(cm^{-1}) = 3190$(m), 3076 (m), 3000(brm), 1638(s), 1583(s), 1528(s), 1480(s), 1438(m), 1381 (brs), 1328(s), 1242(m), 1166(s), 1054(m), 1017(s), 904(w), 878(w), 850(w), 788(s), 712(w), 650(m), 540(m), 438(m). Anal. Calcd. for $C_{20}H_{18}CuN_8O_6$ (529.95), 2: C, 45.33; H, 3.42; N, 21.14. Found: C, 45.65; H, 3.11; N, 19.99 %.

The elemental analysis of carbon, nitrogen, and hydrogen was carried out using an EA1108 (Carlo Erba Instruments, Italy), and the IR spectra were recorded on a BIO RAD FTS 135 spectrometer with KBr pellets.

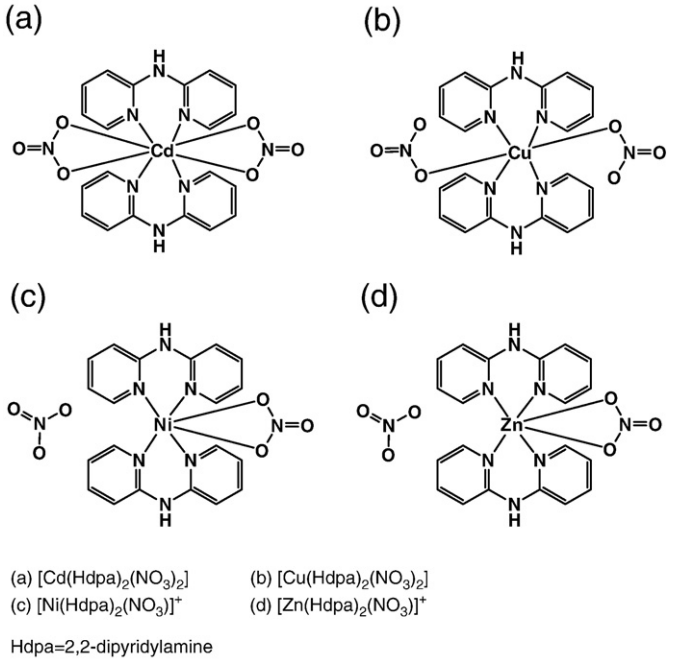

Fig. 1. Molecular structure of $[M(Hdpa)_2(NO_3)_n]^{x+}$ (M = Cd, Cu, Ni, Zn, $n = 1,2$, $x = 1,2$).

2.3. LD as a tool for real-time detection of DNA cleavage

The magnitude of LD in the DNA absorption region depends solely on the flexibility and the length of DNA when the other conditions, including the temperature, concentration, shear gradient, and viscosity are held constant. In double helical DNA, cleaving one of the strand results in increasing the flexibility and cleaving the double strand decreases the contour length of DNA. Both decrease the LD magnitude in the DNA absorption region. Using a previously reported method [20–22], time-dependent LD was recorded at 260 nm right after DNA, $CuCl_2$ and ascorbic were mixed. LD was measured using either a J-715 or a J-810 spectropolarimeter (Tokyo, Japan) and the obtained values were adjusted so that the initial value was 1. A microvolume, thermostatically controlled Couette cell was purchased from (Kromak Ltd., Dunmow, GB) and utilized to orient the DNA sample. The decay of the LD magnitude at 260 nm was determined from the sum of two exponential curves:

$$LD(t) = a_1 \exp(-t/\tau_1) + a_2 \exp(-t/\tau_2) \quad (1)$$

In this equation, the two decay components are assumed to reflect the single and double strand cleavage [20]. The goodness of the analysis was weighed by the weighted residual (D_k), or difference between the measured ($I(t_k)$) and calculated data ($I_c(t_k)$), because it is easier to see the differences between measured and calculated data.

$$D_k = \frac{I(t_k) - I_c(t_k)}{\sqrt{I(t_k)}}$$

For a good fit, these values were expected to be randomly distributed around zero, with a mean value near unity. From this analysis, the reaction time, τ_i, which is inverse of the rate constant for the first order reaction, was obtained. The reaction times were sufficient for comparing each step of multiple processes.

2.4. Cleaving pBR322 super-coiled DNA

Appropriate amounts of $CuCl_2$, ascorbic acid and the metal complexes were added to a super-coiled pBR322 DNA solution in a 5 mM cacodylate buffer (pH7.0) in order to perform the conventional cleavage experiments. The final volume was adjusted to 15 μL for each tube through an addition of a buffer solution, and the final concentration of the super-coiled DNA was 200 ng/15 μL. The mixture was incubated for an hour at 37 °C, and then a loading buffer (7 mM EDTA, 0.15% bromophenol blue, 0.15% xylene cyanol, 75% glycol) was added to stop the reaction. The cleaved products were analyzed in 1%

agarose gel after incubation. The gel was stained in tris-acetate-EDTA (TAE) buffer containing 0.5 μg/mL ethidium bromide, 20 mM tris acetate and 1 mM EDTA. The gel was electrophoresed at 25 V, 400 mA for approximately 400 min. The DNA was visualized using UV trans-illumination and photographed using an Olympus C-5060 camera.

3. Results

3.1. Cleavage of super-coiled DNA probed by electrophoresis

Fig. 2 depicts the gel electrophoresis separations of the metal complex-induced cleavage of pBR322 super-coiled DNA. In lane 1, pBR322 DNA exhibited two clear bands in the absence of the metal complexes, as expected. The intense band corresponded to Form-I (super-coiled form), and the other band corresponded to Form-II (circular DNA). DNA cleavage activity was clearly observed in the presence of $[Cd(Hdpa)_2(NO_3)_2]$ (lanes 2–4, with Cd^{II} complex concentrations of 25 μM (lane 2), 50 μM (lane 3) and 100 μM (lane 4)). At the lowest Cd^{II} complex concentration, the two bands exhibited similar intensities, suggesting that nicked (open circular form, Form II) and cut (linear form, Form III) DNA populations were similar. As the Cd^{II} complex concentration increased (lanes 3 and 4), the intensity of these two bands decreased, which was accompanied by an increase in the intensity of the smeared band. Therefore, shorter DNA resulted from cleavage at more than one place. Similar behavior was observed for $[Cu(Hdpa)_2(NO_3)_2]$ (lanes 5–7). However, the Cu^{II} complex was less effective than the Cd^{II} complex with respect to the overall cleavage of super-coiled DNA. The smeared band was least pronounced for $[Ni(Hdpa)_2(NO_3)]^+$ (lanes 8–10), whereas the bands corresponding to the circular and linear DNA were the most clear out of all of the complexes. The intensity of these two bands was not significantly affected by the concentration of the Ni^{II} complex. The $[Zn(Hdpa)_2(NO_3)]^+$ complex also actively cleaved DNA (lanes 11–13) because the two bands corresponding to Form I and II were clearly visible. The Ze^{II} complex exhibited more effect cleavage with increasing concentration, which was represented by decreases in the intensity of the Form I and II bands as well as an increase in the short fragments.

3.2. Absorption spectra and binding affinities

The binding properties and the affinities of the metal complexes toward double stranded native DNA were investigated using the absorption spectra. In the absence of DNA, all of the complexes produced similar absorption spectra consisting of two main absorption bands at wavelengths below 370 nm. Two maxima peaks at 253 nm and 311 nm, accompanied by two shoulders at ca. 264 nm and 292 nm, were apparent for all of the complexes (data not shown). In Fig. 3(a), the $[Zn(Hdpa)_2(NO_3)]^+$ complexes caused hypochromism

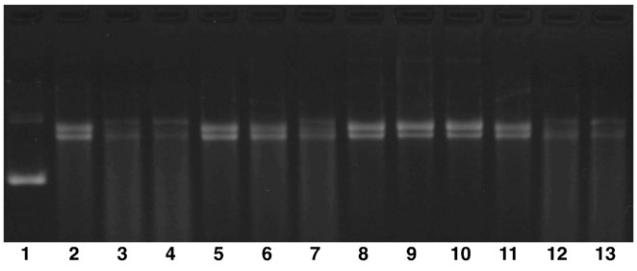

Fig. 2. Cleavage of pBR322 super-coiled DNA by the $[M(Hdpa)_2(NO_3)_n]^{x+}$ complexes detected by gel electrophoresis. Lane 1: DNA alone, [DNA] = 200 ng/μL, lanes 2–4: in the presence of DNA (200 ng/μL), $CuCl_2$ (100 μM), ascorbate (100 μM) and 25 μM (lane 2), 50 μM (lane 3) and 100 μM $[Cd(Hdpa)_2(NO_3)_2]$. Lanes 5–7: the conditions were the same as in lanes 2–4, except for the metal complex, $[Cu(Hdpa)_2(NO_3)_2]$. Lane 8–10: $[Ni(Hdpa)_2(NO_3)]^+$, and lanes 11 ~ 13: $[Zn(Hdpa)_2(NO_3)]^+$.

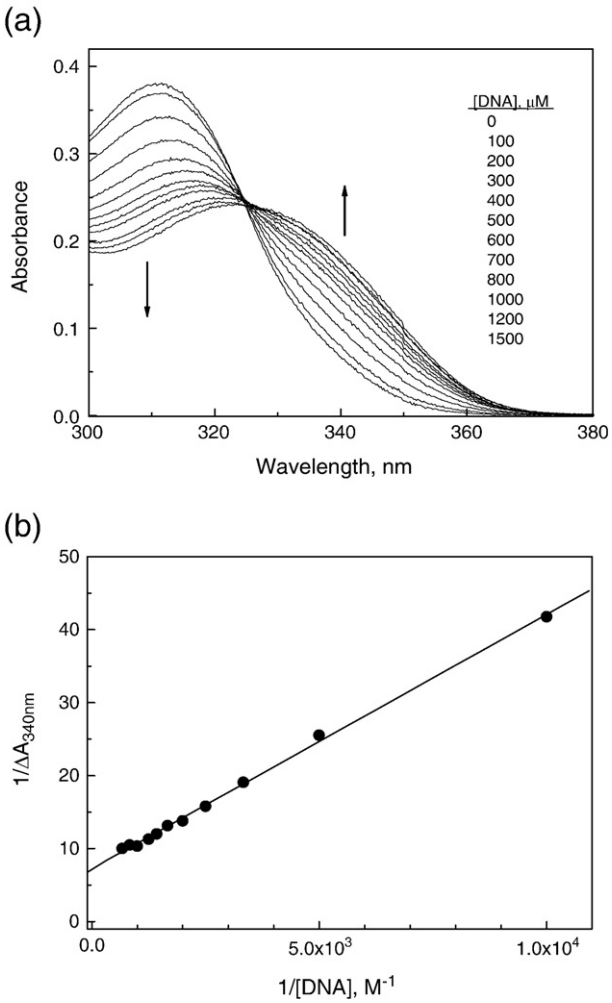

Fig. 3. (a) Absorption spectrum of $[Zn(Hdpa)_2(NO_3)]^+$ in the presence of various concentrations of DNA. The absorption spectrum of DNA was subtracted from the DNA-$[Zn(Hdpa)_2(NO_3)]^+$ complex adducts. [Zn^{II} complex] = 100 μM. (b) An example of the Benesi-Hildebrand plot drawn using the change for the association of the Zn^{II} complex with DNA at 342 nm.

and a red-shift in the lowest energy absorption, which probably corresponded to the metal to ligand charge transfer (MLCT) band. At the highest DNA concentration used in this work (1500 μM), the Zn^{II} complex exhibited 36.8% hypochromism and a ~10 nm red-shift. Other metal complexes produced similar changes in the MLCT absorption band upon binding to DNA (not shown). The changes in absorption spectra indicated that all of the metal complexes interacted with negatively charged DNA regardless of the number of positive charges they carry. Furthermore, an isosbestic point appeared at 324 nm, suggesting that the system consisted of only two metal complex species, the DNA-bound and -unbound metal complexes.

The Benesi–Hildebrand plot was constructed according to the following equation using the changes in the maximum absorbance at a wavelength of 342 nm.

$$\frac{1}{\Delta A_{342\mathrm{nm}}} = -\frac{1}{\left(\varepsilon_b - \varepsilon_f\right)[L_t]} + \frac{1}{\left(\varepsilon_b - \varepsilon_f\right)[L_t]K_{BH}[DNA]}$$

In this equation ε is the molar extinction coefficient, and the subscript b, f and t denote the bound, free and total metal complexes, respectively. $[L_t]$ is the complex concentration and $\Delta A_{342\,\mathrm{nm}}$ is the change in the absorbance at 342 nm. The association constant for the DNA-metal complex adducts formation, K_{BH}, was calculated from

the slope to intercept ratio from the Benesi–Hildebrand plot of the reciprocal absorbance with respect to the reciprocal DNA concentration. The Benesi–Hildebrand plot for the Zn^{II} complex is depicted in Fig. 3(b) as an example. The other complexes produced similar plots and therefore, are not shown. The K_{BH} values for all of the metal complexes are summarized in Table 1. The association constants were in the range of $2.0–2.6\times10^3$, which was not surprisingly high. On the other hand, although the values were within the experimental error, the electrically neutral metal complexes showed tended to have higher association constants than the positively charge complexes.

3.3. The LD measurements

The magnitude of LD reflects the flexibility and the contour length of DNA when the other factors including the viscosity, flow rate and temperature of the sample are held constant as discussed in the experimental section. Therefore, in this experiment, the other factors were held constant in order to determine the changes in the flexibility and contour length from the LD magnitude at 260 nm. Fig. 4(a) shows the LD spectra of the DNA-$Zn(Hdpa)_2(NO_3)_2]^+$ adduct during mixing for the Zn^{II} complex and 30, 60, 120, 180 and 240 min after mixing. Although the intensity changed, the overall shape of LD remained the same even after 240 min, suggesting that the absorption spectrum of the nucleobase was not altered except for the flexibility and the contour length. A slightly negative LD was noticed in the MLCT band of the metal complexes, suggesting that the average electric transition moment of the Zn^{II} complex greatly tilted relative to the DNA helix axis. However, a detailed analysis of the binding geometry could not be carried out because the direction of the transition moment in the MLCT band of the metal complexes was not clear at the current stage and was not in the scope of this study. The intensity of the time-dependent LD spectra decreased with time and the shape was retained, for the other three metal complexes as well, (data not shown). Fig. 4(b) shows the changes in the LD magnitude of the DNA-metal complex adduct at 260 nm with respect to time. In the absence of the metal complex, the LD magnitude of the mixture of DNA, ascorbate, and $CuCl_2$ slowly decreased. The LD magnitude decreased only by *ca.* 10%, 250 after mixing. However, the addition of any one of the four metal complexes resulted in a significant acceleration in the LD magnitude reduction. For instance, the addition of the Cd^{II} complex to the DNA-ascorbate-$CuCl_2$ mixture resulted in almost a complete loss of the LD signal after 240 min (to *ca.* 15%). On the other hand, the LD magnitude decrease was least efficient for the $[Ni(Hdpa)_2(NO_3)]^+$, with a final magnitude of 35% of the initial LD magnitude.

The LD decrease was not explained by simple first order kinetics and instead, consisted of the sum of two exponential decays. Fig. 5 shows an example of the decay curve analysis for the Zn^{II} complex. The goodness of the fit was determined using both the residuals and linear regressions. The decay curve in this particular case consisted of two exponential components, $\tau_1=6.1$ min ($a_1=0.21$) and $\tau_2=34.8$ min ($a_2=0.79$), where a_i was the relative amplitude, and τ_i was the relevant reaction time. The results for the other metal complexes are summarized in Table 1. The decrease in the LD magnitude in the presence of the metal complexes was described by the two exponential decays. The short reaction times were in the range of 6.1 min, for the Zn^{II} complex, to 13.3 min, for the Ni^{II} complex. The long reaction component was between 147.7 min, for the Ni^{II} complex, and 34.8 min for the Zn^{II} complex. The average decay time (reaction time), $\bar{\tau}$, was determined using the equation, $\bar{\tau}=\sum_i a_i\tau_i^2 / \sum_j a_j\tau_j$. The shortest decay time was 33.5 min for the Zn^{II} complex, and the longest time was 141.2 min for the Ni^{II} complex, as expected from the decay curve in Fig. 4(b). The average reaction times for the Cu^{II} and Cd^{II} complexes were 112.0 and 50.8 min, respectively. This kinetic study showed that the Zn^{II} complex induced the fastest DNA cleavage, whereas the Ni^{II} complex was the slowest. Additionally, the Zn^{II} complex most effectively reduced the LD magnitude, 240 min after mixing, whereas the Ni^{II} complex was least effective.

Table 1
Estimated amplitude and reaction time from the time-dependent decrease in the LD magnitude of DNA at 260 nm and the association constant calculated from the Bebesi–Hildebrand plot.

Metal complex	Reaction time (minutes) and amplitude		Binding constant (M^{-1})
$[Cd(Hdpa)_2(NO_3)_2]$	$a_1=0.42$	$\tau_1=8.7$	2.56×10^3
	$a_2=0.58$	$\tau_2=55.6$	
$[Cu(Hdpa)_2(NO_3)_2]$	$a_1=0.34$	$\tau_1=7.1$	2.32×10^3
	$a_2=0.65$	$\tau_2=115.4$	
$[Ni(Hdpa)_2(NO_3)]^+$	$a_1=0.36$	$\tau_1=13.3$	2.05×10^3
	$a_2=0.64$	$\tau_2=147.7$	
$[Zn(Hdpa)_2(NO_3)]^+$	$a_1=0.21$	$\tau_1=6.1$	2.09×10^3
	$a_2=0.79$	$\tau_2=34.8$	

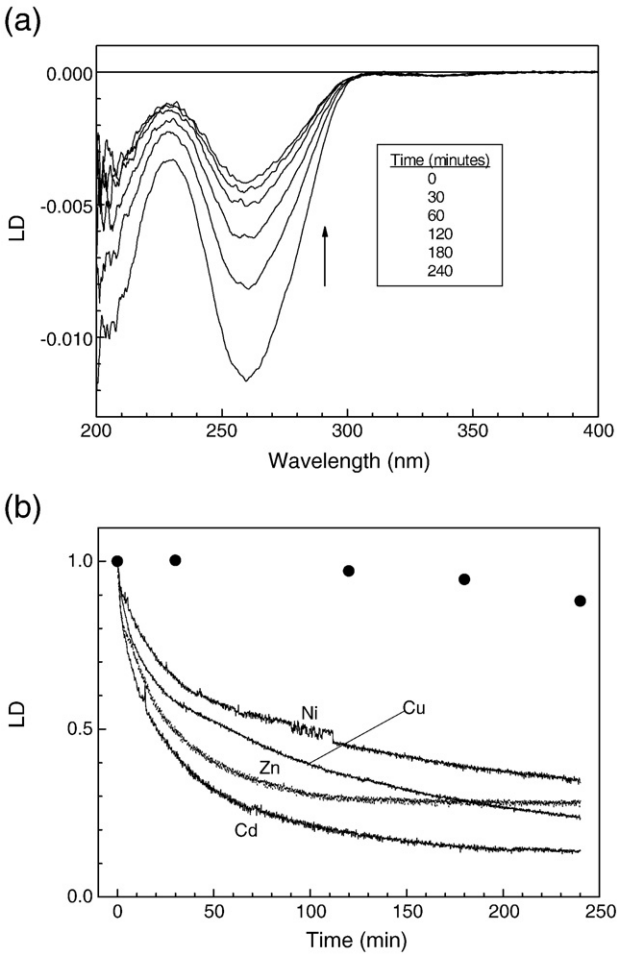

Fig. 4. (a) LD spectrum of $[Zn(Hdpa)_2(NO_3)]^+$ (100 μM) bound to DNA (100 μM) in the presence of $CuCl_2$ (100 μM), and ascorbate (100 μM) with respect to the time during and after mixing. (b) Decrease in the LD intensity at 260 nm with respect to the time after mixing. [DNA] = 200 μM, [Zn^{II} complex] = 100 μM. [$CuCl_2$] = 100 μM, and [ascorbate] = 100 μM.

4. Discussion

The electrophoresis study showed the circular DNA band resulted from single strand nicking, and the linear DNA band from the

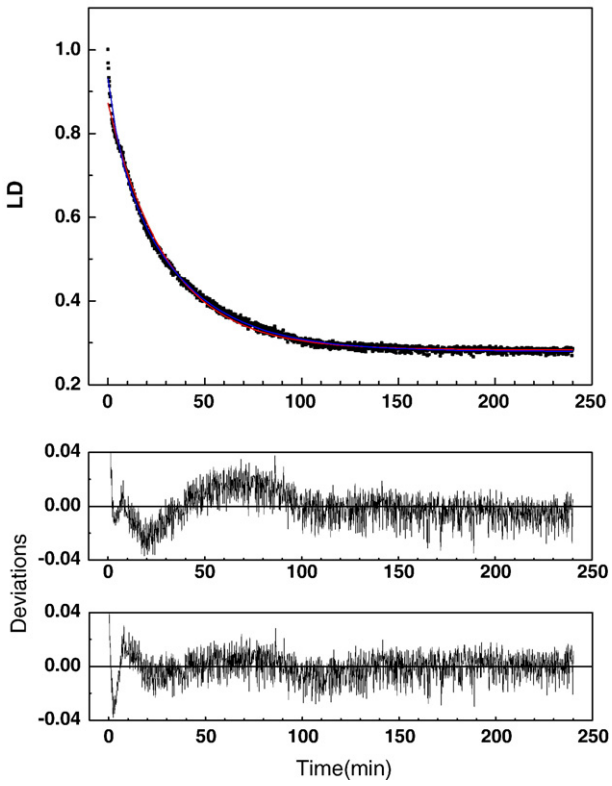

Fig. 5. Measured LD with respect to time at 260 nm as an example of data analysis. $[Zn(Hdpa)_2(NO_3)]^+ = 100$ μM, [DNA] = 200 μM, $[CuCl_2] = 100$ μM, and [ascorbate] = 100 μM. The residuals for the one and two component analyses are also shown in the lower panel. The reaction times and the error range for this particular example are 6.08047 ± 0.30192 and 34.79308 ± 0.24308 min.

scission of both strand. Therefore, all of the metal complexes that were investigated in this study possessed catalytic properties for the DNA cleavage reaction. The appearance of the smeared band in addition to the other two bands, suggested that the cleavage occurred not only at one place but at multi-places, leading to the production of short DNA fragments. Indeed, the amount of circular and linear DNA was negligibly small in the presence of the Cd^{II} and Zn^{II} complexes at the highest concentrations. On the other hand, the strand scission caused by the Ni^{II} complex seemed to occur at one place, and the intensities of the bands representing smeared DNA were too small to detect.

The reduced LD spectrum was determined from the measured LD divided by the isotropic absorption spectrum and was related to the angle, α, between the electric transition moment of the DNA-bound compound and the DNA helix axis using the following equation [24–26]:

$$LD^r(\lambda) = \frac{LD(\lambda)}{A_{iso}(\lambda)} = S \times O = 1.5S\left(<3\cos^2\alpha> -1\right)$$

In this equation, the optical factor, O, was related to the chromophore properties and the angle of the electric transition moment of the given chromophore with respect to the DNA helix axis or the flow-direction in the flow orientation system. This optical factor was assumed to be constant throughout the entire process based on the similar DNA spectra that were observed during mixing and after cleavage (data not shown), which suggested that the changes in the optical properties of the nucleobase (chromophore) were not significant. Furthermore, the relative flexibility and the contour length were measured using LD because the absorption spectrum was constant during mixing and after cleavage. With a constant optical factor, the orientation factor (S), which was the orientation ability of DNA in the flow, solely governed the magnitude of DNA-LD in this study with a constant solvent, temperature and flow rate during the measurements. The orientation ability of DNA in the flow was affected by two factors, the flexibility/rigidity and the contour length of DNA. Cleaving one of the strands of double helical DNA induced bending or kinking at the cleaved site, which, in turn, increased the flexibility of DNA and consequently, reduced the magnitude of DNA-LD. Cleavage near or at the same site of the second strand shortened DNA, which also reduced the magnitude of LD. The presence of the metal complexes certainly accelerated the cleavage of double stranded DNA, which decreased the LD magnitude at a rate that was best described in terms of two exponential decay curves. As described in the previous paragraph, the decrease in the LD magnitude involved the fast single strand cleavage and slow double strand cleavage. This cleavage reaction was most efficiently accelerated by the Zn^{II} complex, with an average reaction time shorter than one third of the reaction time induced by the Ni^{II} complex. The order of efficiency for the metal complexes was $Zn^{II} > Cd^{II} > Cu^{II} > Ni^{II}$, with Zn^{II} as the most efficient.

Considering the crystal structure of the complex [27–29], the Cd^{II} and Cu^{II} complexes were similar, with two NO_3 groups ligated to the central metal atom, whereas Ni^{II} and Zn^{II} had two oxygen atoms of one NO_3 moiety with a +1 charge. Therefore, neither the structure of the complex nor the charge was the main reason for the different efficiencies during the DNA cleavage. The adduct formation abilities of the metal complexes with DNA were obtained from the Benesi–Hildebrand method and were in the same range from approximately 2.0×10^3 to 2.6×10^3. Similar association constants were measured for the metal complexes and were not directly related the charge. Particularly, despite the Zn^{II} complex had the highest cleavage efficiency, whereas the Ni^{II} complex had the lowest, despite the two complexes having the same association constant. Therefore the difference in the DNA cleavage activities was not influenced the binding abilities of the metal complexes or their charge.

Therefore, the structures of the complexes (similar for Zn^{II} and Ni^{II} and for Cd^{II} and Cu^{II}), the charge (Zn^{II} and Ni^{II} were +1 and Cd^{II} and Cu^{II} were neutral), and the binding affinity toward DNA (all complexes exhibited similar binding affinities) did not explain the efficiency order. One possible explanation for the different reactivities was the redox properties of the central metals of the complexes because Cd and Zn are redox-inactive, and Cu and Ni are redox-active [30,31]. Therefore, the Zn and Cd complexes possibly catalyzed the DNA cleavage through hydrolysis, whereas the Cu and Ni complexes carried out DNA cleavage through an oxidative mechanism produced a reactive oxygen species. Based on these results, the hydrolytic DNA cleavage mechanism was more effective than the oxidative cleavage mechanism. Another explanation for order of the DNA cleavage efficiency was the electron configuration of the central metal ions. Both the Zn and Cd atoms belong to group 12. Therefore, the electron configuration at the ground state is $d^{10}s^2$. On the other hand, Cu belongs to group 11 possessing an electron configuration of $d^{10}s^1$, and Ni is a group 10 with an electron configuration of d^8s^2. However, the exact mechanism for the different DNA cleavage efficiency was not clear during this study. Detailed mechanistic studies are currently under investigation to further examine this mechanism.

5. Conclusion

The $[M(Hdpa)_2(NO_3)_n]^{x+}$ (M = Zn^{II}, Cd^{II}, Cu^{II} and Ni^{II}, $n = 1,2$, and $x = 0$, 1) complexes exhibited catalytic effects on the DNA cleavage, and were effectively monitored using LD technique in real-time. The cleavage reaction efficiency with respect to the complex followed the order of $Zn^{II} > Cd^{II} > Cu^{II} > Ni^{II}$, where Zn^{II} was the most effective.

Acknowledgement

This work was supported by an internal Research Grant of Yeungnam University.

References

[1] C.X. Zhang, S.J. Lippard, New metal complexes as potential therapeutics, Curr. Opin. Chem. Biol. 7 (2003) 481–489.
[2] J.A. Cowan, Chemical nucleases, Curr. Opin. Chem. Biol. 5 (2001) 634–642.
[3] J.R. Morrow, O. Iranzo, Synthetic metallonucleases for RNA cleavage, Curr. Opin. Chem. Biol. 8 (2004) 192–200.
[4] L.J.K. Boerner, J.M. Zaleski, Metal complex–DNA interactions: from transcription inhibition to photoactivated cleavage, Curr. Opin. Chem. Biol. 9 (2005) 135–144.
[5] M.E. Núñez, J.K. Barton, Probing DNA charge transport with metallointercalators, Curr. Opin. Chem. Biol. 4 (2000) 199–206.
[6] E.M. Boon, J.K. Barton, Charge transport in DNA, Curr. Opin. Struct. Biol. 12 (2002) 320–329.
[7] B.W. Lee, S.J. Moon, M.R. Youn, J.H. Kim, H.G. Jang, S.K. Kim, DNA mediated resonance energy transfer from 4′, 6-diamidino-2-phenylindole to [Ru(1, 10-phenanthroline)2 L]2+, Biophys. J. 85 (2003) 3865–3871.
[8] B.H. Yun, J.O. Kim, B.W. Lee, P. Lincoln, B. Nordén, J.-M. Kim, S.K. Kim, Simultaneous binding of Ru(II)[(1, 10-phenanthroline)2dipyridophenazine]2+ and minor groove binder 4′, 6-diamidino-2-phenylindole to poly[d(A-T)2] at high binding densities, J. Phys. Chem. B. 107 (2003) 9858–9864.
[9] J.Y. Choi, J.-M. Lee, H. Lee, M.J. Jung, S.K. Kim, J.M. Kim, Mixing ratio-dependent energy transfer from DNA-bound 4′, 6-diamidino-2-phenylindole to [Ru(1, 10-phenanthroline)2dipyrido[3, 2-a:2′, 3′-c]phenazine]2+, Biophys. Chem. 134 (2008) 56–63.
[10] Y.J. Jang, B.-H. Kwon, B.-H. Choi, C.H. Bae, M.S. Seo, W. Nam, S.K. Kim, Intercalation of bulky Δ, Δ- and Λ, Λ-bis-Ru(II) complex between DNA base pairs, J. Inorg. Biochem. 102 (2008) 1885–1891.
[11] J.M. Kim, K.-M. Lee, J.Y. Choi, H.M. Lee, S.K. Kim, The light switch effect upon the association of [Ru(1, 10-phenanthroline)2dipyrido[3, 2-a:2′, 3′-c]phenazine]2+ with single stranded poly(dA) and poly(dT), J. Inorg. Biochem. 101 (2007) 1386–1393.
[12] P. Nordall, F. Westerlund, L.M. Wilhelmsson, B. Nordén, P. Lincoln, Kinetic recognition of AT-rich DNA by ruthenium complexes, Angew. Chem. Int. 46 (2007) 2203–2206.
[13] F. Westerlund, P. Nordall, J. Blechinger, T.M. Santos, B. Nordén, Complex DNA binding kinetics resolved by combined circular dichroism and luminescence analysis, J. Phys. Chem. B 112 (2008) 6688–6694.
[14] J.L. García-Giménez, M. González-Álvarez, M. Liu-González, B. Macías, J. Borrás, G. Alzuet, Toward the development of metal-based synthetic nucleases: DNA binding and oxidative DNA cleavage of a mixed copper(II) complex with N-(9H-purin-6-yl)benzenesulfonamide and 1, 10-phenantroline. Antitumor activity in human Caco-2 cells and Jurkat T lymphocytes. Evaluation of p53 and Bcl-2 proteins in the apoptotic mechanism, J. Inorg. Biochem. 103 (2009) 923–934.
[15] C.H. Ng, H.K.A. Ong, C.W. Kong, K.W. Tan, R. Rahman, B.M. Yamin, S.W. Ng, Factors affecting the nucleolytic cleavage of DNA by (N, N′-ethylenendiaminediacetato) metal(II) complexes, M(edda). Crystal structure of Co(edda), Polyhedron 25 (2006) 3118–3126.
[16] S.S. Ghosh, P.S. Eis, K. Blumeyer, K. Fearon, D.P. Millar, Real time kinetics of restriction endonuclease cleavage monitored by fluorescence resonance energy transfer, Nucleic Acids Res. 22 (1994) 3155–3159.
[17] U. Kettling, A. Koltermann, P. Schwille, M. Eigen, Real-time enzyme kinetics monitored by dual-color fluorescence cross-correlation spectroscopy, Proc. Natl. Acad. Sci. U. S. A. 95 (1998) 1416–1420.
[18] M. Rarbach, U. Kettling, A. Koltermann, M. Eigen, Dual-color fluorescence cross-correlation spectroscopy for monitoring the kinetics of enzyme-catalyzed reactions, Methods 24 (2001) 104–116.
[19] D.A. Hiller, J.M. Fogg, A.M. Martin, J.M. Beechem, N.O. Reich, J.J. Perona, Biochemistry 42 (2003) 14375–14385.
[20] W. Wang, G.J. Lee, K.J. Jang, T.S. Cho, S.K. Kim, Real-time detection of Fe·EDTA/H_2O_2 induced DNA cleavage by linear dichroism, Nucleic Acids Res. (2008) 1–7, doi:10.1093/nar/gkn370.
[21] M.R. Hicks, A. Rodger, C.M. Thomas, S.M. Batt, T.R. Dafforn, Restriction enzyme kinetics monitored by UV linear dichroism, Biochemistry 45 (2006) 8912–8917.
[22] A. Gabibov, E. Yakubovskaya, M. Lukin, P. Favorov, A. Reshetnyak, M. Monastyrsky, Catalytic transforma tions of supercoiled DNA as studied by flow linear dichroismtechnique, FEBS J. 272 (2005) 6336–6343.
[23] A. Rodger, B. Nordén, Circular dichroism and linear dichroism, Oxford University Press, Oxford, 1997.
[24] B. Nordén, M. Kubista, T. Kurucsev, Linear dichroism spectroscopy of nucleic acids, Q. Rev. Biophys. 25 (1992) 51–170.
[25] B. Nordén, T. Kurucsev, Analysing DNA complexes by circular and linear dichroism, J. Mol. Recognit. 7 (1994) 141–156.
[26] Y. Matsuoka, B. Nordén, Linear dichroism studies of nucleic acids. II. Calculation of reduced dichroism curves of A-and B-form DNA, Biopolymer 21 (1982) 2433–2452.
[27] H. Kwak, S.H. Lee, S.H. Kim, Y.M. Lee, E.Y. Lee, B.K. Park, E.Y. Kim, C. Kim, S.-J. Kim, Y. Kim, Construction of Zn^{II} compounds with a chelating 2,2′-dipyridylamine (Hdpa) ligand: Anion effect and catalytic activities, Eur. J. Inorg. Chem. (2008) 408–415.
[28] B.K. Park, G.H. Eom, S.H. Kim, H. Kwak, S.M. Yoo, Y.J. Lee, C. Kim, S.-J. Kim, Y. Construction of Cd(II) compounds with a chelating ligand 2, 2′-dipyridylamine (Hdpa): anion effect, catalytic activities and luminescence, Polyhedron 29 (2010) 773–786.
[29] Personal communications: Crystal structures of [Ni(Hdpa)2(NO3)]+and [Cu (Hdpa)2(NO3)2] have been determined by Dr. Youngmee Kim at Department of Chemistry and Nono Science in Ewha Womans University in Korea. Cu complex has a similar structure to Cd complex and Ni complex to Zn as shown in Figure 1.
[30] E. Kim, E.E. Chufan, K. Kamaraj, K.D. Karlin, Synthetic models for heme-copper oxidases, Chem. Rev. 104 (2004) 1077.
[31] Y.J. Song, H. Kwak, Y.M. Lee, S.H. Kim, S.H. Lee, B.K. Park, J.Y. Jun, S.M. Yu, C. Kim, S.-J. Kim, Y. Kim, Metal-directed supramolecular assembly of metal(II) benzoates (M = Co, Ni, Cu, Zn, Mn, and Cd) with 4,4′-bipyridine: effects of metal coordination modes and novel catalytic activities, Polyhedron 28 (2009) 1241–1252 (and reference therein).